Applied Clay Science 158 (2018) 29–36

Contents lists available at ScienceDirect

Applied Clay Science

journal homepage: www.elsevier.com/locate/clay

Research paper

Smectite formation upon lime stabilization of expansive marls

Kerstin Elert[a,*], José Miguel Azañón[b,c], Fernando Nieto[a,c]

[a] Department of Mineralogy and Petrology, University of Granada, Fuentenueva S/N, Granada 18002, Spain
[b] Department of Geodynamics, University of Granada, Fuentenueva S/N, Granada 18002, Spain
[c] IACT, CSIC-University of Granada, Spain

ARTICLE INFO

Keywords:
Soil stabilization
Smectites
C-(A)-S-H
Dolomitic lime
Carbonation

ABSTRACT

Marl was treated with Mg-rich lime to evaluate the effectiveness of lime stabilization for this expansive, clay- and carbonate-rich material. XRD and TEM analyses revealed very limited dissolution of expandable clay minerals and neoformation of Mg-enriched smectites. C-(A)-S-H phases formed and initially cemented clay particles. However, they experienced decalcification and decomposition over time, leading to disaggregation of clay particles and deterioration of some of the marl's geotechnical properties. Results question the effectiveness of lime stabilization for marls, especially using Mg-rich lime. Modifications to commonly used treatment protocols in order to overcome these shortcomings are discussed.

1. Introduction

Lime stabilization has been used to improve the plastic properties of subgrades for almost a century (Bell, 1996). Generally, lime stabilization is performed to reduce the soil's plasticity index and swelling capacity, both being related to the presence of large amounts of smectites in highly plastic soils. In the case of clayey soils, lime treatments often proved successful (Al-Mukhtar et al., 2010; Di Sante et al., 2014). However, doubts have been recently raised regarding the effectiveness of lime stabilization for marls, containing important amounts of carbonates (Sol-Sánchez et al., 2016). In this case, common lime treatment protocols may result in premature stabilization failure. To overcome the shortcomings of lime treatments for marls, alternative stabilization agents (i.e., fly- and biomass-ash, and Ca-rich industrial or mine waste) have been tested (Ureña et al., 2015).

The addition of lime to soils provokes several reactions which include: a) reduction in the soils´ moisture content due to the hydration of lime (I. $CaO + H_2O \rightarrow Ca(OH)_2$); b) reduction of intracrystalline swelling due to cation-exchange in soils containing Na-smectites; c) reduction of osmotic swelling as a result of lower clay particle repulsion in the presence of an electrolyte (flocculation); d) precipitation of calcium carbonate and/or binding of soil particles upon carbonation of portlandite (II. $Ca(OH)_2$ (s) + CO_2 (g) + H_2O (aq) → $CaCO_3$ (s) + $2H_2O$ (aq) + heat ↑ (74 kJ/mol) (Moorehead, 1986)); e) dissolution of clay minerals and other mineral phases (i.e., feldspars and quartz) and the formation of pozzolanic materials (i.e., C-(A)-S-H, calcium (aluminum) silicate hydrates) with high cementing capacity and mechanical strength (Bell, 1996).

Mineral dissolution and pozzolanic phase formation are of special importance in order to achieve particle aggregation and improve the soil's geotechnical characteristics. Upon dissolution, aluminosilicate minerals (i.e., clays) provide Al and Si species for the formation of pozzolanic phases (Gaucher and Blanc, 2006). Clay minerals show different dissolution rates in alkaline environments, depending on layer charge, structure, and chemical composition. Generally, illite has been found to dissolve more slowly than kaolinite and smectite (Carroll and Starkey, 1971; Jozefaciuk and Bowanko, 2002). From a geotechnical point of view a reduction of the smectite content due to dissolution would be highly desirable. However, in our previous study only a very minor decrease in the smectite content (i.e., smectite being the dominant clay mineral of the tested marl) was detected and permanent particle aggregation was not achieved in marl treated with calcitic or Mg-rich lime (Elert et al., 2017). Consequently, initially improved geotechnical properties started to deteriorate over time (Ureña et al., 2015).

In order to determine possible mineralogical changes other than the limited dissolution of clay minerals and formation of C-(A)-S-H, which could explain the observed stabilization failure, exhaustive additional analyses were performed. In the current study we focused on the effects of Mg-rich lime for marl stabilization. Mg-rich lime is widely used for soil stabilization and is the most common lime exploited in the USA (Boynton, 1984). It is also very abundant in the area of Granada (southern Spain), where problems associated with expansive marl have been reported (Azañón et al., 2010). Furthermore, marl treatment with Mg-rich lime is more likely to produce detectable compositional changes in smectites upon neoformation, because Mg^{2+} is expected to

* Corresponding author.
E-mail address: kelert@ugr.es (K. Elert).

https://doi.org/10.1016/j.clay.2018.03.014
Received 16 November 2017; Received in revised form 1 March 2018; Accepted 6 March 2018

partially replace Al^{3+} in the octahedral layer of smectites, whereas Ca^{2+} from calcitic lime would only enter as an interlayer cation.

The results obtained here point to a transformation, rather than a destruction of smectite clay minerals. This unexpected finding has important implications in the field of civil engineering and might lay the basis for the modification of current treatment protocols, especially in the case of post-stabilization failure.

2. Materials and methods

2.1. Materials

The marl sample was extracted from clay-rich levels at 32 m depth from the base of the Diezma landslide (southern Spain), responsible for important structural damage to the A-92 highway back in 2001 (Azañón et al., 2010). This material belongs to a Flysch-type formation outcropping continuously in the western and central parts of the Betic Cordillera (Bourgois et al., 1974). According to X-ray diffraction (XRD), the untreated marl contained clay minerals (predominantly smectite and small amounts of kaolinite and mica), quartz, calcite and minor amounts of feldspar and dolomite. Elemental analysis (EA) revealed a carbonate content of 24.4%, and thermogravimetric (TG) analysis of ethylene glycol (EG) solvated samples (Nieto et al., 2008) gave an average smectite content of 30.5 ± 2.0 wt% in the untreated marl (Elert et al., 2017).

The Mg-rich lime was obtained from residual sludge from the local extraction of magnesium-rich limestone and marble. This sludge was calcined and hydrated prior to its use and contained 54.21 wt% CaO and 25.26 wt% MgO as well as trace amounts of SiO_2, Al_2O_3, and Fe_2O_3 according to X-ray fluorescence analysis (Elert et al., 2017). Considering a loss on ignition of 18.60 wt%, it was concluded that the hydrated lime only contained an insignificant amount of carbonates and was, therefore, expected to be highly reactive.

2.2. Sample preparation

Hundred fifty grams of dry marl sample was mixed with 15 wt% of dry Mg-rich lime and thoroughly mixed for 10 min. A sufficient amount of water was added until the plastic limit was reached. The sample was kept in the laboratory exposed to air at room *T*. Water was added when needed in order to keep the sample completely covered and to limit carbonation. Aliquots were taken at 7, 14, 21, 49, 77, 105, and 201 days. The treated marl was stirred prior to the collection of aliquots in order to obtain a homogeneous sample.

2.3. Analytical methods

pH measurements were performed periodically during the lime treatment using a pH-meter Stick Piccolo HI 1280 with ± 0.1 pH accuracy (Hanna Instruments).

A laser particle size analyzer (Mastersizer 2000LF, Malvern Instruments) was used to determine the particle size distribution of untreated and treated marl samples dispersed in alcohol.

Surface area measurements (BET method (Brunauer et al., 1938)) were performed on untreated and treated soil samples using a TriStar 3000 analyzer (Micrometrics). Prior to analysis, samples were degassed at 80 °C for 24 h using a sample degas system (VacPrep 061, Micrometrics). Degassing was performed at such a relatively low *T* in order to avoid changes in the smectite structure.

Mineralogical changes upon lime treatment were studied with a PANanalytical X'Pert Pro X-ray diffractometer using disoriented powder samples. Equipment settings: CuKα radiation, 45 kV, 40 mA, 5–70° 2Θ exploration range, 0.008° 2ϴ step size, and 10 s/step counting time. Xpowder software (Martín-Ramos, 2004) was used to identify mineral phases.

The smectite content was determined by TG analysis according to the methodology developed by Nieto et al. (2008), consisting in weight loss (WL) measurements of EG solvated and Mg saturated samples in a *T* range between 100 and 450 °C. The smectite content was calculated according to the following equation: Sme% = 3.96 WL − 4.05.

Field emission scanning electron microscopy (FESEM, Auriga (Carl Zeiss) was used to determine morphological and microstructural changes upon lime treatment. Carbon coated samples were analyzed at 3 kV beam accelerating voltage in secondary electron imaging mode.

Transmission electron microscopy (TEM) was performed on untreated and treated marl samples using two microscopes. A Philips CM20 was used for quantitative elemental analysis (TEM-AEM) in scanning transmission electron microscopy (STEM) mode coupled to an EDAX solid-state energy dispersive X-ray (EDX) detector. Equipment settings: 200 kV accelerating voltage and 20 × 100 nm scan window. Images and compositional maps were obtained using a Titan (FEI) with XFEG emission gun, spherical aberration corrector and High Angle Annular Dark Field (HAADF) detector working at 300 kV. Powdered samples were dispersed in ethanol, sonicated, and deposited on C-coated Cu grids. Mineral standards were used to obtain k-factors according to the method by Cliff and Lorimer (1975).

3. Results and discussion

3.1. Physical properties and pH evolution

Particle size distribution analyses revealed that the average particle size of untreated marl was 10 μm. It increased by 70% immediately after 15 wt% Mg-rich lime was added (Fig. 1). Concomitantly, the surface area of the marl sample decreased from 39 m^2/g to 14 m^2/g. These changes can be attributed to flocculation, which is a pH-independent process. Actually, no drop in pH was observed at this point. The presence of an electrolyte, which includes most salts, bases, and acids, facilitates the flocculation of colloidal clay particles. Flocculation is achieved by reducing the range of electrical double layer repulsion between particles (van Olphen, 1987). These particles aggregate into larger clusters and, consequently, experience a surface area decrease (Mowafy et al., 1985), as was observed in the marl sample treated here.

After 1 week of treatment, the particle size and surface area increased by 124 and 146%, respectively. Both effects can be correlated with the formation of C-(A)-S-H phases (Elert et al., 2017). FESEM images (Fig. 2) confirmed the aggregation of clay particles and the formation of new phases, possibly C-(A)-S-H), in samples treated for 1 week. C-(A)-S-H phases have high cementing capacity and result in the formation of large, relatively stable aggregates of clay particles, leading to the observed particle size increase (Fig. 1). They generally

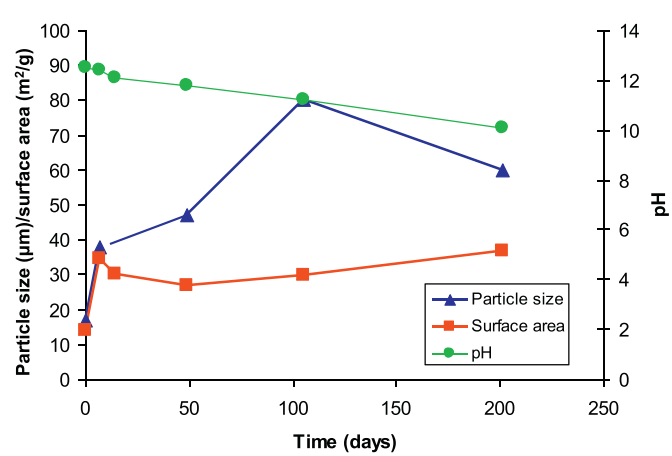

Fig. 1. pH evolution, particle size and surface area of marl treated with 15 wt% Mg-rich lime for 201 days. The surface area and particle size of the untreated marl were 39 m^2/g and 10 μm, respectively.

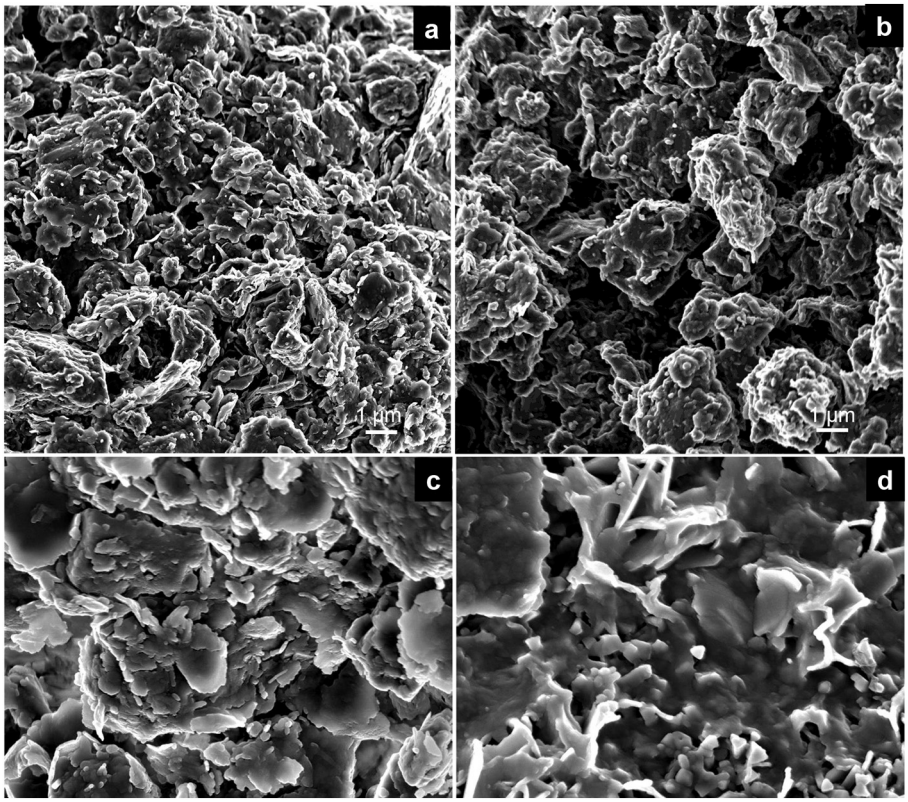

Fig. 2. FESEM image of a) and c) untreated marl, b) marl treated for 7 days with 15 wt% Mg-rich lime, showing aggregated clay particles, and d) marl treated for 105 days with 15 wt % Mg-rich lime, showing newly formed, gel-like phases (possibly C-(A)-S-H).

have very large surface areas due to a significant volume fraction of internal nano-pores (Jennings et al., 2008), which explains the important surface area increase detected here after 1 week. Upon further treatment, the surface area showed some variations, but a clear tendency could not be established. Particle size continued to increase until 105 days of treatment, indicating further cementation of clay particles. More prolonged treatment induced a disaggregation of clay particles which was manifested by a 20% decrease in average particle size after 201 days of treatment. Note that the trend regarding particle size and specific surface area evolution was not particular to the soil sample treated with 15 wt% lime but was also observed in samples treated with 10 wt% Mg-rich lime (Elert et al., 2017). Disaggregation was, most likely, induced by the decomposition of C-(A)-S-H as the pH decreased (see below).

Our experimental results revealed that the initial pH of the lime-treated soil decreased from ~12.5 to 10.1 after 201 days (Fig. 1). At this pH, C-(A)-S-H seemed to be no longer stable, which is in agreement with (Frizon et al., 2009), who stated that the stability range of most cement hydrates, including C-S-H, falls between pH 12.5 and 10.5. The reason for the pH decrease is twofold. On the one hand, $Ca(OH)_2$ reacts with atmospheric CO_2 to form $CaCO_3$ (reaction II), the equilibrium pH of $CaCO_3$ being 9. On the other hand, dissolution of aluminum silicates and C-(A)-S-H formation consume OH-groups and, thus, contributes to the pH decrease (Gaucher and Blanc, 2006). It could be argued that the remaining $Mg(OH)_2$ in the Mg-rich lime, which is difficult to carbonate, would sustain a sufficiently high pH as to prevent the decomposition of C(A)SH phases, and/or to favor clay dissolution. However, the pH of a saturated $Mg(OH)_2$ solution is only 10.5 (25 °C). A reduction in pH during lime treatment is inevitable and independent of the soil's mineralogical composition. The high carbonate content in marls, however, causes a faster pH decrease as compared to clayey soils. According to Berner (1992), marl-type groundwater resulted in a much faster C-S-H degradation as compared to pure water. Faster degradation takes place in the presence of carbonates due to their action as a pH buffer, hampering a pH increase. The lower pH associated with the presence of carbonates has an important influence on the effectiveness of lime treatments for soil stabilization. Numerous studies (Köhler et al., 2005; Huertas et al., 2009) have shown that clay mineral dissolution rates decrease drastically at pH < 11. Thus, the amount of Al and Si species available for the formation of pozzolanic phases will decrease as well. Additionally, C-(A)-S-H phases decompose as pH decreases (Aguilera et al., 2003; Baston et al., 2012), mostly due to carbonation. A practical example of the devastating action of atmospheric CO_2 or carbonate-bearing water on C-(A)-S-H phases was brought upon by Hodgkinson and Hughes (1999) who studied the mortars of the Hadrian's wall, UK. These authors found that poorly ordered C-(A)-S-H phases were still detectable in 1700 year old Roman mortar in compact zones which prevented carbonation. In more porous and more degraded zones, however, these phases were completely carbonated.

3.2. Mineralogical evolution of lime treated marl

XRD analysis of marl treated with 15 wt% Mg-rich lime revealed that mineral dissolution occurred within the first 7 days, resulting in a small, but noticeable decrease in intensity of the 001 reflection of smectite, mica and kaolinite (Fig. 3). A clear change in the intensity of the general *(hkl)* reflection of phyllosilicates at 4.46 Å, however, was not observed. Portlandite was not detected after 7 days of treatment. It had either transformed into C-(A)-S-H upon reaction with dissolved Al and Si species or into calcite upon carbonation. Brucite, in contrast, was still present even after 201 days, indicating a slow carbonation as a result of its low solubility (Lanas et al., 2006). The intensity of the 104 reflection of dolomite decreased upon treatment, probably due to de-dolomitization. Dedolomitization involving the reaction of dolomite with portlandite to form calcite and brucite (III. $CaMg(CO_3)_2 + Ca(OH)_2 \rightarrow 2CaCO_3 + Mg(OH)_2$) has previously been observed in

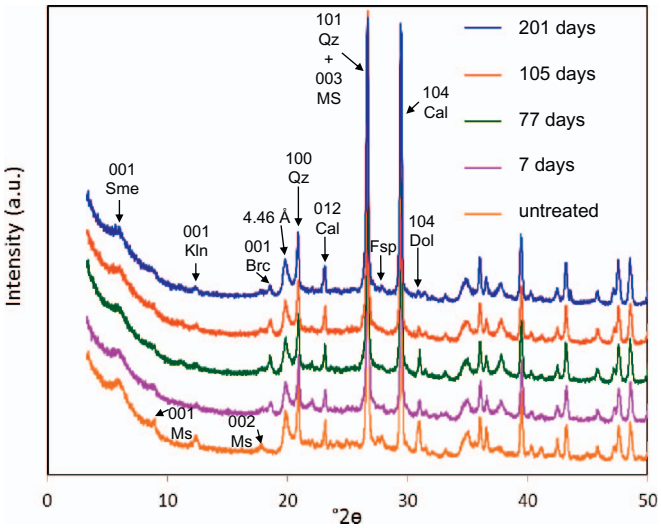

Fig. 3. XRD patterns of non-oriented powder samples of untreated marl sample and marl treated with 15 wt% Mg-rich lime for up to 201 days. Sme = smectite, Kln = kaolinite, Ms = unspecified micas, Brc = brucite, 4.46 Å = general (*hkl*) reflection of phyllosilicates, Qz = quartz, Cal = calcite, Fsp = feldspar, Dol = dolomite. Mineral symbols after Whitney and Evans (2010).

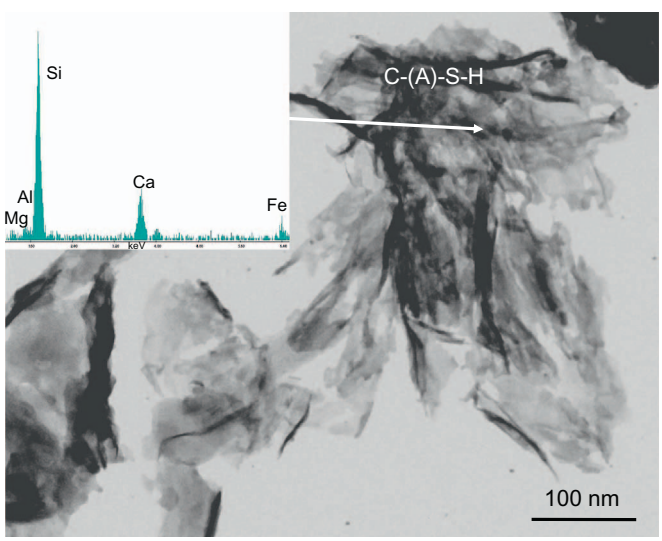

Fig. 4. TEM image of gel-like C-(A)-S-H in a marl sample treated with 15 wt% Mg-rich lime for 201 days. EDX-microanalysis in inset.

dolomitic repair mortars (Lanas et al., 2006). Evidence for the presence of C-(A)-S-H phases could not be provided by XRD analysis, suggesting an amorphous character of this phase consistent with its gel-like appearance observed using FESEM (Fig. 2) and TEM (Fig. 4). Overall, XRD results suggest that only the fine-grained fraction of the marl suffered dissolution which included clay minerals, quartz, feldspars, and dolomite. This is in agreement with findings by Huertas et al. (1999), showing a preferential dissolution of fine-grained material in the case of kaolinite exposed to alkaline conditions. XRD results were confirmed by TG measurements of EG solvated marl samples, revealing an only insignificant reduction in smectites from 30.5 ± 2 wt% in untreated marl to 29.2 ± 2.3 wt% in marl treated with 15 wt% Mg-rich lime. Note that this minor change in the smectite content falls within the error of this technique (Nieto et al., 2008).

3.2.1. Compositional changes in smectites

The smectites of the untreated marl were identified as members of the beidellite-montmorillonite solid solution series, with some nontronitic component (Elert et al., 2017). The treatment with 15 wt % Mg-rich lime for 201 days produced a Mg increase with a concomitant decrease in octahedral Al in smectites (Table 1). The tetrahedral Si content and the sum of octahedral cations, in contrast, remained basically unchanged. The observed changes indicate a transformation of smectites as a result of dissolution and precipitation reactions undergone by the treated marl. Phase diagrams (Fig. 5) revealed that the increase in octahedral Mg occurred after only 7 days of treatment and further augmented over the course of the treatment, whereas the reduction in octahedral Al took place more gradually. The early Mg increase caused an apparent transitory increase in the octahedral occupancy. However, at least part of the excess octahedral occupancy might actually be attributed to interlayer Mg. In smectites, Mg can be present both, in the octahedral and in the interlayer positions. According to Sánchez-Roa et al. (2018), in the case of environments particularly rich in Mg a coherent formula of smectites can only be adjusted if part of the Mg is considered as interlayer cations. In the case of the smectite studied here, Mg entered more easily in the interlayer space during the first stage of the lime treatment until a reduction in octahedral Al enabled the entry of Mg in the octahedral sheet.

The presence of Mg is crucial for the formation of smectites. Kloprogge et al. (1999) stated that even montmorillonite which only contains a small amount of Mg, would need Mg for its formation. Remarkably, a reanalysis of TEM-AEM data of marl treated with 15 wt% calcitic lime (data reported in Elert et al., 2017), also revealed a neoformation of smectites with increased Mg content. In this case the small amount of dolomite present in the original marl served as the Mg source (Fig. 3), following its partial dissolution under the alkaline treatment conditions (Elert et al., 2017). Our TEM-AEM analyses also show that even after 201 days of treatment, some smectite particles had a chemical composition close to that of the untreated smectite (Table 1). Note that these analyses also provided evidence for cation exchange upon lime treatment and the interlayer Ca^{2+} increased by ~45%, partially replacing K^+ (Table 1). The only partial replacement of K^+ is not unexpected. It is known that K^+ is not easily replaced by Ca^{2+} due to the higher hydration energy of the latter (Shawney, 1972).

These TEM-AEM results yield important information which helps explain the deterioration of physical and geotechnical properties observed in lime-treated marls over time (Ureña et al., 2015; Elert et al., 2017). Apparently, the lime treatment did not only fail to destroy important amounts of smectites (Elert et al., 2017), but also resulted in the precipitation of new smectitic clay minerals with higher Mg concentration. It might even be speculated that the fine fraction of the non-swelling clay minerals (i.e., micas and kaolinite) and other phases such as feldspars were actually transformed into smectites (Churchman and Lowe, 2011).

3.2.2. Compositional changes of C-S-H phases

C-(A)-S-H phases form relatively rapid in lime treated soils (Al-Mukhtar et al., 2010; Di Sante et al., 2014). Our previous TEM analyses revealed the presence of these pozzolanic phases after only 1 week in marls treated with calcitic lime (Elert et al., 2017). C-(A)-S-H phases were also detected in samples treated with Mg-rich lime. Fig. 6 shows C-(A)-S-H interspersed with clay minerals and carbonates in samples treated with 15 wt% Mg-rich lime for 201 days. The selected area electron diffraction (SAED) pattern of C-(A)-S-H did not reveal any well-defined spots or Debye rings but produced diffuse haloes which are typical for amorphous phases (Fig. 6, inset). Remarkably, the Ca/Si ratio decreased from 0.55 in samples treated for 49 days (pH = 11.8) to 0.37 in samples treated for 201 days (pH = 10.1) due to the decalcification (i.e., preferential Ca leaching during dissolution) of C-(A)-S-H phases, leading to their deterioration. This process has been identified as a common cause of concrete degradation (Ashraf, 2016). Note that complete decalcification will lead to the decomposition of C-S-H into $CaCO_3$ and silica gel, resulting in a strength decrease and the formation of macroporosity (Dauzeres et al., 2016). Results presented by

Table 1
Structural formulae (TEM-AEM) of smectite (based on $O_{10}(OH)_2$) from untreated marl and marl treated with 15 wt% Mg-rich lime for 201 days.

	Si	Al^{IV}	Al^{VI}	Mg	Fe	Σ Oct.[a]	K	Ca	Σ Int.[b]
Smectite from untreated marl									
	3.68	0.32	1.32	0.21	0.46	1.99	0.46	0.05	0.56
	3.56	0.44	1.21	0.26	0.53	2.00	0.44	0.14	0.72
	3.81	0.19	1.21	0.36	0.43	2.01	0.24	0.14	0.52
	3.56	0.44	1.47	0.12	0.52	2.11	0.09	0.07	0.22
	3.63	0.37	1.12	0.28	0.63	2.03	0.31	0.12	0.56
	3.77	0.23	1.34	0.21	0.47	2.01	0.16	0.12	0.40
	3.82	0.18	1.43	0.19	0.35	1.97	0.29	0.09	0.47
	3.90	0.10	1.20	0.19	0.56	1.96	0.00	0.21	0.41
	3.71	0.29	1.33	0.21	0.44	1.98	0.42	0.07	0.56
	3.89	0.11	1.36	0.30	0.26	1.92	0.47	0.09	0.65
	3.70	0.30	1.48	0.17	0.38	2.04	0.16	0.10	0.36
	4.02	0.00	1.34	0.19	0.39	1.92	0.10	0.12	0.34
	3.74	0.26	1.13	0.30	0.59	2.02	0.24	0.12	0.49
	3.81	0.19	1.39	0.24	0.38	2.02	0.17	0.10	0.38
	3.84	0.16	1.10	0.24	0.64	1.98	0.17	0.14	0.45
	3.98	0.02	1.31	0.29	0.36	1.97	0.21	0.10	0.41
	3.99	0.01	1.15	0.31	0.52	1.97	0.12	0.14	0.40
	3.76	0.24	1.45	0.23	0.33	2.00	0.24	0.10	0.45
Average	3.79	0.21	1.30	0.24	0.46	1.99	0.24	0.11	0.46
	± 0.14	± 0.13	± 0.13	± 0.06	± 0.11	± 0.04	± 0.14	± 0.04	± 0.12
Smectite with changed composition after 201 days of treatment									
	3.90	0.10	1.03	0.43	0.54	2.00	0.16	0.19	0.54
	3.56	0.44	0.85	0.78	0.56	2.19	0.23	0.21	0.65
	4.00	0.00	1.10	0.38	0.53	2.01	0.15	0.09	0.33
	3.74	0.26	0.83	0.58	0.66	2.07	0.24	0.19	0.63
	3.76	0.24	1.29	0.39	0.33	2.01	0.44	0.07	0.58
	3.84	0.16	1.11	0.35	0.51	1.97	0.30	0.16	0.61
	4.03	0.00	1.16	0.36	0.40	1.92	0.14	0.17	0.48
	3.93	0.07	0.89	0.65	0.49	2.03	0.31	0.16	0.63
	3.64	0.36	1.54	0.35	0.26	2.14	0.00	0.14	0.28
	4.06	0.00	0.97	0.52	0.48	1.97	0.1	0.14	0.38
	3.86	0.14	0.92	0.57	0.59	2.08	0.00	0.24	0.48
	4.04	0.00	1.07	0.43	0.43	1.93	0.07	0.21	0.48
	3.65	0.35	1.17	0.58	0.44	2.19	0.16	0.10	0.37
Average	3.85	0.16	1.07	0.49	0.48	2.04	0.18	0.16	0.50
	± 0.17	± 0.15	± 0.20	± 0.13	± 0.11	± 0.09	± 0.13	± 0.05	± 0.12
Smectite with unchanged composition after 201 days of treatment									
	3.69	0.31	1.37	0.28	0.35	2.00	0.37	0.11	0.58
	3.78	0.22	1.61	0.23	0.17	2.01	0.42	0.00	0.42
	4.02	0.00	1.16	0.29	0.47	1.92	0.12	0.17	0.47
	3.79	0.21	1.66	0.17	0.16	1.98	0.12	0.16	0.43
Average	3.82	0.19	1.45	0.24	0.29	1.98	0.26	0.11	0.48
	± 0.14	± 0.13	± 0.23	± 0.06	± 0.15	± 0.04	± 0.16	± 0.08	± 0.07

[a] Sum of octahedral cations.
[b] Sum of interlayer charge.

Sasaki and Saeki (2007) are in agreement with our data, showing a similar decrease in the Ca/Si ratio as the pH of the lime-treated marl decreased. According to Thiery et al. [2011] decalcification is especially pronounced in the case of C-(A)-Si-H phases with low Ca/Si ratios as those detected here. After 201 days, the chemical composition of C-(A)-S-H phases did not differ significantly from those found in samples treated with calcitic lime for the same period of time by Elert et al. (2017) and TEM-AEM analyses showed an almost constant Ca/Si ratio (Table 2). Remarkably, the Mg concentration in these phases was either very low or zero. This result is in agreement with previous findings, showing no or very little Mg uptake in C-S-H gel (Lothenbach et al., 2015). Recent studies (Chiang et al., 2014; Lothenbach et al., 2015) suggest that the existence of a solid solution series between C-S-H and M-S-H gel is not very likely due to differences in the structure of C-S-H and M-S-H as well as in the ionic radius of Ca^{2+} and Mg^{2+}.

3.3. Implications of mineralogical changes on the geotechnical performance of lime-treated marl

The neoformation of smectites and the decomposition of C-(A)-S-H phases upon lime treatment can have important implications on the geotechnical performance of marls. Ureña et al. (2015) found that the addition of 2% lime caused an initial improvement in the geotechnical properties of the tested marl, which however started to reverse after only 6 months when the plasticity index and free swelling increased and the California bearing ratio (CBR, i.e., penetration test to evaluate mechanical strength of subgrades) decreased.

The increase in swelling capacity can be explained with the neoformation of smectites and, more importantly, with the decomposition of C-(A)-S-H phases, resulting in clay particle disaggregation. Disaggregated smectite particles offer a larger surface area for water absorption and will thus regain part of their swelling capacity. The reduction in mechanical strength in lime-treated marl is, as in the case of Portland cement (Huet et al., 2010), related to the decomposition of C-(A)-S-H, demonstrated here by the decalcification of these phases detected after 201 days. However, several modifications to the lime stabilization process might improve the efficacy of the treatment and overcome some of its shortcomings.

1) The formation of a sufficient amount of pozzolanic phases is critical in order to achieve a long-term improvement in the marl's geotechnical properties. Since pozzolanic reactions require water in order to promote mineral dissolution, additional or prolonged wetting

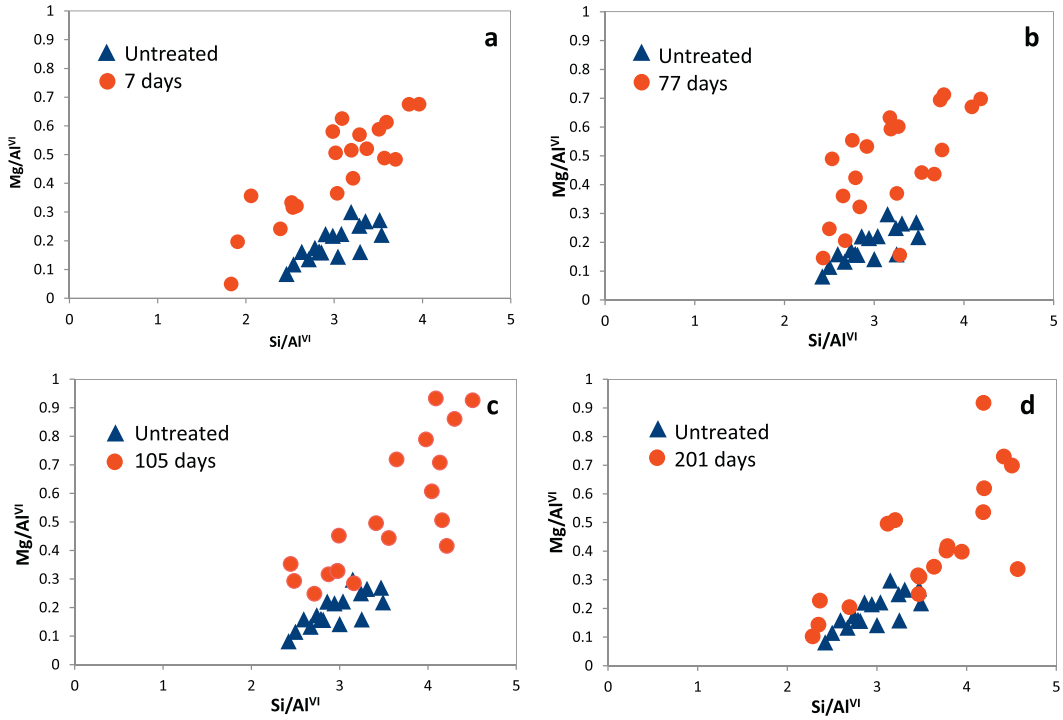

Fig. 5. Evolution of Mg/Al^{VI} and Si/Al^{VI} ratios in marl samples treated with 15 wt% Mg-rich lime for up to 201 days.

of lime treated soil would be beneficial to obtain larger amounts of C-S-H phases. Maintaining sufficiently high soil moisture content during lime treatment would also reduce carbonation by limiting the diffusion of atmospheric CO_2 in water-saturated pores (Cizer et al., 2010). Adapting the treatment schedule to seasonal climate conditions, especially in southern European countries, would also be beneficial to avoid rapid drying during hot summer months. Treatments during cold winter months should also be avoided since pozzolanic reactions are halted at low temperatures (Bell, 1996).

2) Maintaining a high pH is essential to facilitate mineral dissolution and avoid carbonation of C-S-H phases. Obviously, higher lime concentrations will provide additional OH^- available for reaction over a longer period of time (Deneele et al., 2016). However, eventually pH will drop as a result of mineral dissolution, C-S-H formation, and carbonation of $Ca(OH)_2$ and C-S-H. The addition of a small amount of KOH might overcome this shortcoming. KOH has an equilibrium pH of > 13 and not only enhances mineral dissolution, but also facilitates the formation of non-swelling, relatively stable materials (i.e., zeolites or zeolite precursors) with cementing properties (Elert et al., 2015). Furthermore, illitization of smectites could be induced in the presence of potassium, which would reduce the clay's swelling capacity (Drief et al., 2002).

3) According to results by Hodgkinson and Hughes (1999), C-S-H phases were protected from carbonation in more compact zones of 1700-year old Roman mortar. Thus, additional compaction during lime treatment might hinder the access of carbonated ground water and atmospheric CO_2 and prevent C-S-H phases from decomposing into $CaCO_3$ and silica gel.

4. Conclusions

Analytical results revealed the neoformation of Mg-rich smectites at an early stage of the lime treatment and the decomposition of C-(A)-S-H phases over time, which led to the deterioration of the marl's geotechnical properties (i.e., increased swelling capacity and mechanical strength reduction).

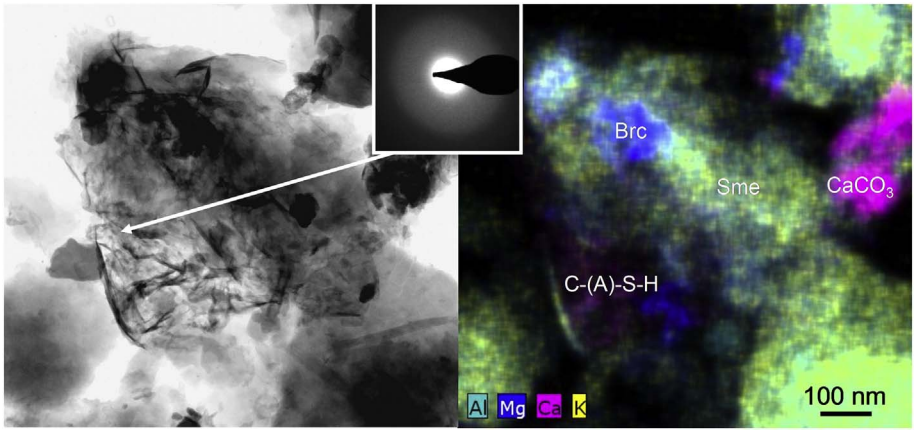

Fig. 6. HAADF-TEM image and element map of C-(A)-S-H interspersed with smectite (Sme) particles, calcite (Cal) and brucite (Brc) in a marl sample treated with 15 wt% Mg-rich lime for 201 days. Inset shows SAED pattern of amorphous C-(A)-S-H.

Table 2
Composition (TEM-AEM data) of C-(A)-S-H phases from marl treated with 15 wt% Mg-rich lime for 49 and 201 days.

	Si	Ca	Mg	Al	Fe
C-(A)-S-H composition after 49 days					
	1.00	0.47	0.08	0.13	0.09
	1.00	0.61	0.03	0.08	0.04
	1.00	0.30	0.10	0.06	0.03
	1.00	0.53	0.04	0.09	0.07
	1.00	0.55	0.03	0.08	0.04
	1.00	0.58	0.04	0.05	0.07
	1.00	0.56	0.00	0.04	0.04
	1.00	0.53	0.00	0.06	0.03
	1.00	0.50	0.03	0.05	0.04
	1.00	0.52	0.01	0.04	0.06
	1.00	0.54	0.04	0.11	0.07
	1.00	0.59	0.00	0.05	0.05
	1.00	0.52	0.01	0.06	0.03
	1.00	0.61	0.04	0.06	0.06
	1.00	0.54	0.02	0.07	0.07
Average	1.00	0.55	0.03	0.07	0.05
	± 0.00	± 0.04	± 0.02	± 0.03	± 0.02
C-(A)-S-H composition after 201 days					
	1.00	0.54	0.00	0.03	0.00
	1.00	0.32	0.00	0.00	0.06
	1.00	0.36	0.10	0.06	0.00
	1.00	0.38	0.00	0.02	0.00
	1.00	0.35	0.00	0.04	0.00
	1.00	0.36	0.03	0.04	0.00
	1.00	0.22	0.07	0.07	0.07
	1.00	0.34	0.03	0.06	0.13
	1.00	0.47	0.00	0.00	0.04
	1.00	0.40	0.00	0.00	0.04
Average	1.00	0.37	0.02	0.03	0.03
	± 0.00	± 0.09	± 0.04	± 0.03	± 0.04

The fact that neoformation of smectite is related to the presence of Mg^{2+}, points to a limited effectiveness of lime treatments for soils containing dolomite and questions the use of Mg-rich lime for soil stabilization in general.

It might be argued that destabilization of C-(A)-S-H phases upon pH decrease, would be especially severe in marl's due to their high carbonate content, acting as a pH buffer and not apply to clayey soils. However, a similar pH decrease due to mineralogical changes (i.e., mineral dissolution, formation of C-(A)-S-H, and carbonation of Ca $(OH)_2$ and C-(A)-S-H)) can also be expected in lime-treated clayey soils, even though at a lower reaction rate.

Overall the efficacy of lime stabilization treatments for marls (and clayey soils) might be improved by modifying conventional protocols, including a prolongation of the wetting phase during treatment, additional compaction, and the use of additives such as KOH.

Acknowledgement

The authors thank the personnel of the Centro de Instrumentación Científica (University of Granada) for assistance with TEM, FESEM, TG, and particle size analysis. We are grateful to Dr. Carlos Rodriguez Navarro for the revision of the manuscript.

References

Aguilera, J., Blanco-Varela, M.T., Martinez-Ramirez, S., 2003. Thermodynamic modelling of the CaO-SiO2-CaCO3-H2O closed and open system at 25 °C. Mater. Constr. 53, 35–43.
Al-Mukhtar, A., Lasledj, A., Alcover, J.-F., 2010. Behaviour and mineralogy changes in lime-treated expansive soil at 20 °C. Appl. Clay Sci. 50, 191–198.
Ashraf, W., 2016. Carbonation of cement-based materials: challenges and opportunities. Constr. Build. Mater. 120, 558–570.
Azañón, J.M., Azor, A., Yesares, J., Tsige, M., Mateos, R.M., Nieto, F., Delgado, J., López-Chicano, M., Martín, W., Rodríguez-Fernández, J., 2010. Regional-scale high-plasticityclay-bearing formation as controlling factor on landslides in Southeast Spain. Geomorphology 120, 26–37.
Baston, G.M.N., Clacher, A.P., Heath, T.G., Hunter, F.M.I., Smith, V., Swanton, S.W., 2012. Calcium silicate hydrate (C-S-H) gel dissolution and pH buffering in a cementitious near field. Mineral. Mag. 76, 3045–3053.
Bell, F.G., 1996. Lime stabilization of clay minerals and soils. Eng. Geol. 42, 223–237.
Berner, U.R., 1992. Evolution of pore water chemistry during degradation of cement in a radioactive waste repository environment. Waste Manag. 12, 201–219.
Bourgois, J., Chauve, P., Didon, J., 1974. La formation d'argiles a blocs dans la province de Cadix, Cordilleras Betiques, Espagne. Reun. Annu. Sci. Terre 2, 79.
Boynton, R.S., 1984. Lime and limestone. In: Encyclopaedia of Chemical Technology, 3rd ed. Wiley, New York.
Brunauer, S., Emmett, P.H., Teller, E., 1938. Adsorption of gases in multimolecular layers. J. Am. Chem. Soc. 60, 309–319.
Carroll, D., Starkey, H.C., 1971. Reactivity of clay minerals with acids and alkalines. Clay Clay Miner. 19, 321–333.
Chiang, W.-S., Ferraro, G., Fratini, E., Ridi, F., Yeh, Y.-Q., Jeng, U.-S., Chen, S.-H., Baglioni, P., 2014. Multiscale structure of calcium- and magnesium-silicate-hydrate gels. Mater. Chem. A 2, 12991–12998.
Churchman, G.J., Lowe, D.J., 2011. Alteration, formation, and occurance of minerals in soils. In: Huang, P.M., Li, Y., Summer, M.E. (Eds.), Handbook of Soil Sciences, 2nd edition. Properties and Processes, vol. 1. CRC Press (Taylor and Francis), Boca Raton, pp. 20.1–20.72.
Cizer, Ö., van Balen, K., van Gemert, D., 2010. Competition between hydration and carbonation in hydraulic lime and lime-pozzolana mortars. Adv. Mater. Res. 133-134, 241–246.
Cliff, G., Lorimer, G.W., 1975. The quantitative analysis of thin specimens. J. Microsc. 103, 203–207.
Dauzeres, A., Achiedo, G., Nied, D., Bernard, E., Alahrache, S., Lothenbach, B., 2016. Magnesium perturbation in low-pH concretes placed in clayey environment – solid characterization and modeling. Cem. Concr. Res. 79, 137–150.
Deneele, D., Le Runigo, B., Cui, Y.-J., Cuisinier, O., Ferber, V., 2016. Experimental assessment regarding leaching of lime-treated silt. Constr. Build. Mater. 112, 1032–1140.
Di Sante, M., Fratalocchi, E., Mazzieri, F., Pasqualini, E., 2014. Time of reactions in a lime treated clayey soil and influence of curing conditions on its microstructure and behavior. Appl. Clay Sci. 99, 100–109.
Drief, A., Martinez-Ruiz, F., Nieto, F., Velilla Sanchez, N., 2002. Transmission electron microscopy evidence for experimental illitization of smectite in K-enriched seawater solution at 50 °C and basic pH. Clay Clay Miner. 50, 746–756.
Elert, K., Sebastian, E., Rodriguez-Navarro, C., 2015. Alkaline activation as an alternative method for the consolidation of earthen architecture. J. Cult. Herit. 16, 461–469.
Elert, K., Nieto, F., Azañón, J.M., 2017. Effects of lime treatments on marls. Appl. Clay Sci. 135, 611–619.
Frizon, F., Gin, S., Jegou, C., 2009. Mass transfer phenomena in nuclear waste packages. In: Wang, L. (Ed.), Advances in Transport Phenomena. Springer-Verlag, Berlin.
Gaucher, E.C., Blanc, P., 2006. Cement/clay interactions – a review: experiments, natural analogues, and modeling. Waste Manag. 26, 776–788.
Hodgkinson, E.S., Hughes, C.R., 1999. The mineralogy and geochemistry of cement/rock reactions: high-resolution studies of experimental and analogue materials. In: Metcalfe, R., Rochelle, C.A. (Eds.), Chemical Containment of Waste in the Geosphere. Geol. Soc. London Spec. Pub 157pp. 195–211.
Huertas, F.J., Chou, L., Wollast, R., 1999. Mechanism of kaolinite dissolution at room temperature and pressure: part II kinetic study. Geochim. Cosmochim. Acta 63, 3261–3275.
Huertas, F.J., Hidalgo, A., Rozalen, M.L., Pellicione, S., Domingo, C., Garcia Gonzalez, C.A., Andrade, C., Alonso, C., 2009. Interaction of bentonite with supercritically carbonate concrete. Appl. Clay Sci. 42, 488–496.
Huet, B.M., Prevost, J.H., Scherer, G.W., 2010. Quantitative reactive transport modeling of Portland cement in CO2-saturated water. Int. J. Greenh. Gas Control 4, 561–574.
Jennings, H.M., Bullard, J.W., Thomas, J.J., Andrade, J.E., Chen, J.J., Scherer, G.W., 2008. Characterization and modelling of pores and surfaces in cement paste: correlations to processing and properties. J. Adv. Concr. Technol. 6, 5–29.
Jozefaciuk, G., Bowanko, G., 2002. Effect of acid and alkali treatments on surface áreas and adsorption energies of selected minerals. Clay Clay Miner. 50, 771–783.
Kloprogge, J.T., Komarneni, S., Amonette, J.E., 1999. Synthesis of smectite clay minerals: a critical review. Clay Clay Miner. 47, 529–554.
Köhler, S.J., Bosbach, D., Oelkers, E.H., 2005. Do clay mineral dissolution rates reach steady state? Geochim. Cosmochim. Acta 69, 1997–2006.
Lanas, J., Perez Bernal, J.L., Bello, M.A., Alvarez, J.I., 2006. Mechanical properties of masonry repair dolomitic lime-based mortars. Cem. Concr. Res. 36, 951–960.
Lothenbach, B., Nied, D., Hopital, E.L., Achiedo, G., Dauzeres, A., 2015. Magnesium and calcium silicate hydrates. Cem. Concr. Res. 77, 60–68.
Martín-Ramos, J.D., 2004. Using XPowder: A Software Package for Powder X-Ray Diffraction Analysis. (GR 1001/04. ISBN 84-609-1497-6).
Moorehead, D.R., 1986. Cementation by the carbonation of hydrated lime. Cem. Concr. Res. 16, 700–708.
Mowafy, Y.M., Bauer, G.E., Sakeb, F.H., 1985. Treatment of expansive soils: a laboratory study. Transp. Res. Rec. 1032, 34–39.
Nieto, F., Abad, I., Azañón, J.M., 2008. Smectite quantification in sediments and soils by thermogravimetric analysis. Appl. Clay Sci. 38, 288–296.
van Olphen, H., 1987. Dispersion and flocculation. In: Newman, A.C.D. (Ed.), Chemistry of Clay Minerals. Mineralogical Society Monograph No. 6 Longman Scientific & Technical, London, pp. 203–224.
Sánchez-Roa, C., Bauluz, B., Nieto, F., Abad, I., Jimenéz-Millán, J., Faulkner, D., 2018. Micro- and nano-scale study of deformed phyllosilicate-rich gouges from the Galera Fault Zone (Betic Cordillera, SE Spain). Am. Miner (in press).

Sasaki, K., Saeki, T., 2007. Effect of chemical composition of C-S-H on concrete. J. Soc. Mater. Sci. Jpn. 56, 699–706.
Shawney, B.L., 1972. Selective sorption and fixation of cations by clay minerals: a review. Clay Clay Miner. 20, 93–100.
Sol-Sánchez, M., Castro, J., Ureña, C.G., Azañón, J.M., 2016. Stabilization of clayey and marly soils using industrial wastes: pH and laser granulometry indicators. Eng. Geol. 200, 10–17.
Thiery, M., Faure, P., Morandeau, A., Platret, G., Bouteloup, J.-F., Dangla, P., Baroghel-Bouny, V., 2011. Effect of carbonation on the microstructure and moisture properties of cement-based materials. In: International Conference on Durability of Building Materials and Components, Porto. Portugal, pp. 1–8.
Ureña, C., Azañón, J.M., Corpas, F.A., Salazar, L.M., Ramírez, A., Rivas, F., Mochón, I., Sierra, M.J., 2015. Construcción de un terraplén con suelo estabilizado mediante el uso de agentes alternativos en la Autovía del Olivar. Carreteras 63–72.
Whitney, D.L., Evans, B.W., 2010. Abbreviations for names of rock-forming minerals. Am. Miner. 95, 185–187.